Jurnal Teknologi

Full Paper

# THE DYNAMIC EFFECTS OF PIEZOELECTRIC ACCELEROMETER ON THE STABILITY OF AN ACTIVE VIBRATION CONTROL SYSTEM

Muhajir Ab. Rahim*, Fathinul Syahir Ahmad Sa'ad, Ammar Zakaria

School of Mechatronic Engineering, Universiti Malaysia Perlis, 02600 Arau, Perlis, Malaysia

*Corresponding author
muhajir@unimap.edu.my

**Article history**
Received
*1 June 2015*
Received in revised form
*13 July 2015*
Accepted
*20 August 2015*

**Graphical abstract**

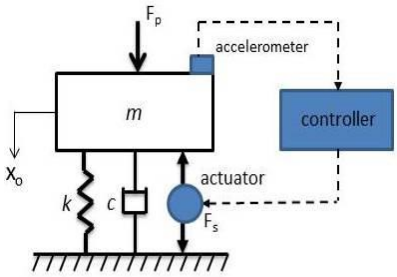


## Abstract

The main purpose of this work is to study the dynamic effects of a piezoelectric accelerometer in an active vibration control system. The analysis is focused on the stability based on Nyquist stability criterion. This is done by deriving the overall open-loop system transfer function for a single-degree-of-freedom system which includes the sensor dynamics into the equation. The polar plot results show that the system is only unconditionally stable for acceleration, but is conditionally stable for velocity and displacement feedback control.

*Keywords*: Piezoelectric accelerometer, active vibration control, Nyquist stability

## Abstrak

Tujuan utama kerja ini ialah untuk mengkaji kesan dinamik meter pecut piezoelektrik dalam sistem kawalan getaran aktif. Analisa difokuskan kepada kestabilan berdasarkan kriteria kestabilan Nyquist. Ini dilakukan dengan menerbitkan rangkap pindah bagi keseluruhan sistem gelung buka untuk darjah kebebasan tunggal yang mengandungi dinamik penderia ke dalam persamaan. Plot kutub yang terhasil menunjukkan sistem hanya stabil tak bersyarat bagi kawalan suap balik pecutan, tetapi stabil bersyarat bagi kawalan suap balik halaju dan sesaran.

*Kata kunci*: Meter pecut piezoelektrik, kawalan getaran aktif, kestabilan Nyquist



## 1.0 INTRODUCTION

In recent years, active vibration control has attracted significant amount of attention because of the advantages of this method in reducing vibration of mechanical system over the conventional approach [1-4]. Basically, it consists of three main components which are sensor, controller and actuator. The sensor is used to measure the vibration signal. Meanwhile, the function of the electrical controller is to give command to the actuator. The command signal from the controller to the actuator is based on the sensor measurement input. Thus, the actuator will generate a secondary force such that it can cancel or reduces the excitation force of the vibration by the principle of destructive interference [5].

However, the active vibration control has potential in instability issue [5, 7]. This is mainly due to its electronic instrumentations, as well as the dynamics of applied actuator and sensors. For this reason, the main scope of this work is to study the dynamic effect of a sensor particularly piezoelectric accelerometer in determining the stability of active vibration control system. This analysis will be based on the Nyquist stability criterion, where the overall open-loop transfer function of the system will be derived. Three different control strategies, namely acceleration, velocity and displacement feedback control will be considered. As a result, simple formulae will be derived to determine the frequency at

which the system becomes unstable, and also the maximum gain that could be applied to each system. These formulae will give insight into how the dynamics of piezoelectric govern the instabilities.

## 2.0 THEORETICAL MODEL OF ACTIVE VIBRATION CONTROL SYSTEM

Consider a vibrating mechanical system is being supported by an isolator with stiffness and damping as shown in Figure 1. Initially, the active control is off (secondary force, $f_s=0$) such that the primary force, $f_p$ which is subjected to the mechanical system can be derived as

$$f_P(t) = M\ddot{e}(t) + C\dot{e}(t) + Ke(t) \tag{1}$$

where $C$ is the system's damping, $K$ is the system's stiffness, and $E$ is the displacement of the system's mass, $M$.

Based on (1), the mechanical system transfer function can be expressed as

$$G(s) = \frac{E(s)}{F_p(s)} = \frac{1}{Ms^2 + Cs + K} \tag{2}$$

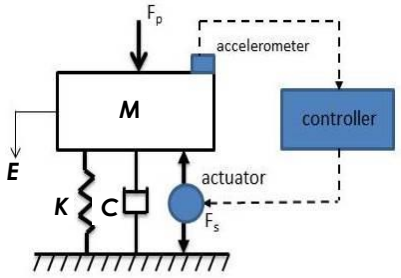


**Figure 1** Single-degree-of-freedom model of active vibration isolation system

By considering piezoelectric accelerometer as the sensor in this study, its basic mechanical model can be assumed as a single-degree-of-freedom of a mass-spring-damper system as shown in Figure 2. Note that, its vibration measurement is based on the relative displacement, $z=y-x$ of piezoelectric mass, $M_s$ to the base on which it is attached.

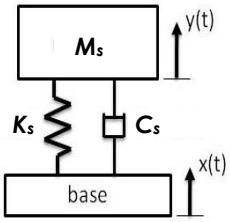


**Figure 2** Mechanical model of piezoelectric accelerometer

Therefore, by applying Newton's second law of motion, the equation of motion of the mass, $M_s$ can be written as

$$M_s\ddot{y} + C_s(\dot{y} - \dot{x}) + K_s(y - x) = 0 \tag{3}$$

where $M_s$ is the sensor mass, $K_s$ is the sensor stiffness and $C_s$ is the sensor damping.

By assuming the vibrating body (base) and the corresponding response are in harmonic motion, such that respectively given by

$$x = X_o e^{j\omega t} \tag{4}$$

$$z = Z_o e^{j\omega t} \tag{5}$$

and substituting (4) and (5) into (3) will give

$$M_s\ddot{z} + C_s\dot{z} + K_s z = -M_s\ddot{x} \tag{6}$$

Then, the relative motion from (6) can be simplified further to obtain

$$Z_o = \frac{M_s s^2 X_o}{M_s s^2 + C_s s + K_s} \tag{7}$$

Since, $s^2 X_o = a_o$ is the base acceleration's magnitude, the accelerometer transfer function can be given by

$$S(s) = \frac{Z_o(s)}{a_o(s)} = \frac{M_s}{M_s s^2 + C_s s + K_s} \tag{8}$$

Note that, the main function of active vibration control is to modify the system response in terms of effective mass, damping and stiffness of the mechanical system [5]. For example, by using acceleration feedback control the effective mass of the mechanical system could be modified. Meanwhile, velocity feedback and displacement feedback control is used to adjust the effective damping and effective stiffness of the mechanical system respectively. Thus, the typical command signal from the controller can be expressed as

$$H(s) = g_a s^2 + g_v s + g_d \tag{9}$$

where $g_a$ is the acceleration control gain, $g_v$ is velocity control gain, and $g_d$ is displacement control gain. In this case, the velocity signal can be found by integrating the acceleration signal from the accelerometer. Meanwhile the displacement signal can be determined by double integration of the acceleration signal.

## 3.0 SYSTEM STABILITY

Figure 3 shows the equivalent block diagram of vibration control by feedback control system as presented in Figure 1. The mechanical response can be expressed as

$$E(s)=G(s)\left[F_P(s)-F_S(s)\right] \tag{10}$$

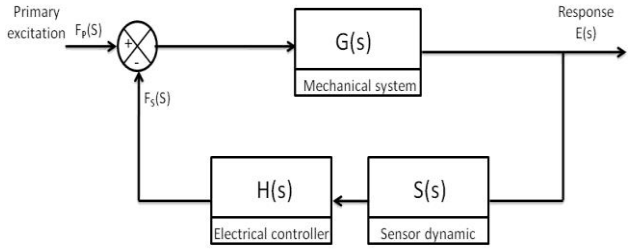


**Figure 3** Equivalent block diagram of vibration control

It shows that, the secondary excitation $F_S(s)$ results from the controller transfer function $H(s)$, sensor transfer function $S(s)$ and the mechanical response $E(s)$, which is $F_S(s)=H(s)S(s)E(s)$. It means that, the controller $H(s)$ will generate large secondary excitation force $F_S(s)$ to cancel the primary excitation $F_P(s)$, if the response $E(s)$ is large, and vice-versa.

Based on the block diagram of Figure 3, the closed transfer function of $E(s)/F_P(s)$ can be obtained such as

$$\frac{E(j\omega)}{F_P(j\omega)}=\frac{G(j\omega)}{1+G(j\omega)S(j\omega)H(j\omega)} \tag{11}$$

where $s=j\omega$ is substituted in (11) in order to transform the equation into frequency response function (FRF).

By assuming that the plant $G(s)$, sensor $S(s)$ and controller $H(s)$ are individually stable, the stability of the closed loop system is assured provided the polar plot of the open-loop frequency response does not encircle the Nyquist critical point (-1,0) which corresponds to the Nyquist stability criterion [6]. It is clear that from (11) the open-loop FRF, $G(j\omega)S(j\omega)H(j\omega)$ plays an important role in the system stability. For example, if the open-loop gain is unity at any frequency $\omega_c$, but there is also $180^0$ open-loop phase shift, so that at $\omega=\omega_c$

$$G(j\omega)S(j\omega)H(j\omega)=-1 \tag{12}$$

Therefore, the system will become unstable since $E(j\omega)\to\infty$, where the mechanical response is approaching infinity at $\omega=\omega_c$. This is indirectly, associated with the open-loop frequency response passing through the critical point (-1,0) at the frequency $\omega_c$. The stability analysis can be clearly seen by plotting the Nyquist or polar plot, which is based on the open-loop transfer function $G(j\omega)S(j\omega)H(j\omega)$.

Accordingly, the system open-loop transfer function can be expressed in non-dimensional frequency as

$$G(j\Omega)S(j\Omega)H(j\Omega)=\frac{M_s}{K_s}\left(\frac{-(g_a/M)\Omega^2+j(2\zeta g_v/C)\Omega+(g_d/K)}{1-\Omega^2+j2\zeta\Omega}\right)\left(\frac{1}{1-\Omega_s^2+j2\zeta_s\Omega_s}\right) \tag{13}$$

In this equation, the plant non-dimensional frequency is given by $\Omega=\omega/\omega_n$ and sensor non-dimensional frequency is $\Omega_s=\omega/\omega_{ns}$, where $\omega_{ns}$ is the sensor natural frequency. In order to generalize this equation into simpler terms, $\alpha$ is introduced. It is the ratio between sensor natural frequency, $\omega_{ns}$ with plant natural frequency $\omega_n$, which is given by

$$\alpha=\frac{\Omega}{\Omega_s} \tag{14}$$

By substituting (14) into (13), results

$$G(j\Omega)S(j\Omega)H(j\Omega)=\frac{M_s}{K_s}\left(\frac{-(g_a/M)\Omega^2+j(2\zeta g_v/C)\Omega+(g_d/K)}{1-\Omega^2+j2\zeta\Omega}\right)\left(\frac{1}{1-(\Omega/\alpha)^2+j2\zeta_s(\Omega/\alpha)}\right) \tag{15}$$

Therefore, the stability for each of acceleration, velocity and displacement feedback control can be derived as the following;

### 3.1 Acceleration Feedback Control

In the case of acceleration feedback control, both of $g_v$ and $g_d$ is set to zero such that (15) can be written as

$$G(j\Omega)S(j\Omega)H(j\Omega)=\frac{-g_aM_s}{MK_s}\left(\frac{\Omega^2}{1-\Omega^2+j2\zeta\Omega}\right)\left(\frac{1}{1-(\Omega/\alpha)^2+j2\zeta_s(\Omega/\alpha)}\right) \tag{16}$$

Based on the Nyquist stability criterion, the system is unstable if the open-loop frequency response encircles the critical point (-1,0). In order to identify system stability, the crossing point of the open-loop transfer function on the real axis is determined by separating (16) into real and imaginary parts respectively as

$$\mathrm{Re}\{G(j\Omega)S(j\Omega)H(j\Omega)\}=\frac{-g_aM_s}{MK_s}\frac{\left((\Omega\alpha)^2\right)\left(\alpha^2-\Omega^2-(\Omega\alpha)^2+\Omega^2\left(\Omega^2-4\zeta\zeta_s\alpha\right)\right)}{\left((1-\Omega)^2+(2\zeta\Omega)^2\right)\left(\left(\alpha^2-\Omega^2\right)^2+(2\zeta_s\Omega\alpha)^2\right)} \tag{17}$$

$$\mathrm{Im}\{G(j\Omega)S(j\Omega)H(j\Omega)\}=\frac{-g_aM_s}{MK_s}\frac{2\Omega^3\alpha^2\left(\zeta\left(\Omega^2-\alpha^2\right)+\zeta_s\alpha\left(\Omega^2-1\right)\right)}{\left((1-\Omega)^2+(2\zeta\Omega)^2\right)\left(\left(\alpha^2-\Omega^2\right)^2+(2\zeta_s\Omega\alpha)^2\right)} \tag{18}$$

Then, by equating the imaginary part in (18) to zero, the critical frequency can be found to occur at $\Omega=0$ and $\sqrt{\alpha(\zeta\alpha+\zeta_s)(\zeta+\alpha\zeta_s)}/(\zeta+\alpha\zeta_s)$. By substituting the critical frequency into real part term in (17), the first crossing point is found at the origin, and the second crossing point is on the positive real axis (assume $g_aM_s/MK_s=1$). This result is illustrated in the polar plot simulations of Figure 4.

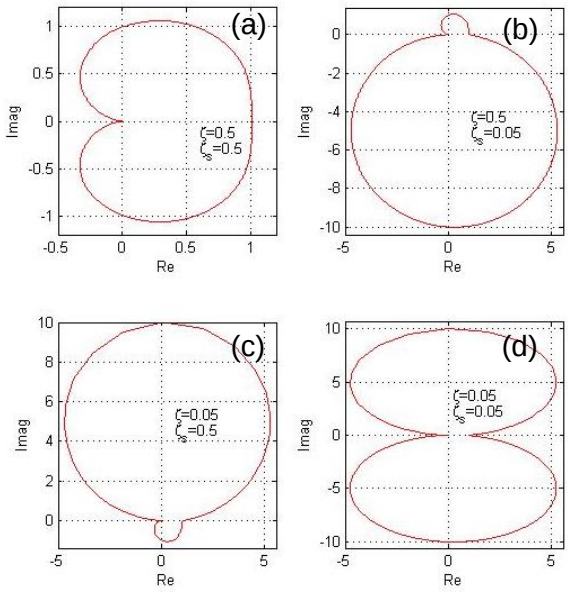


**Figure 4** Polar plot of acceleration feedback control with different values of $\zeta$ and $\zeta_s$

In general, by including the sensor dynamics into the open-loop transfer function, the polar plot will have two loops, instead of single loop that corresponds to the plant dynamics [7]. Note that, the extra loop in Figure 4 represents the sensor dynamics. Yet, it is observed that the system is stable, since there is no crossing point on the negative real axis with the variation values of $\zeta$ and $\zeta_s$. From here, it can be understood that, the shape and size of the plot will change due to effect of changing the values of the damping ratios. For example in Figure 4(b), with a smaller value of sensor damping ratio that is $\zeta < \zeta_s$ the size of the bottom plot that corresponds to the sensor dynamics will become bigger. In contrast, when $\zeta_s$ is larger, its size will become smaller as shown in Figure 4(c).

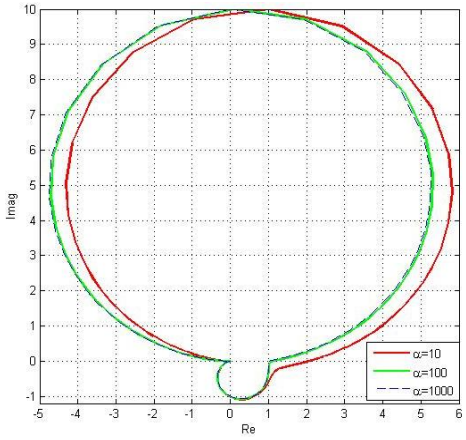


**Figure 5** Polar plot of acceleration feedback control with different values of α

The effect of the variation of *a* is presented in Figure 5. It is clear that, the system still manages to retain its stability. By having higher value of *a*, the polar plot will be closer to the theoretical plot [7]. However, by decreasing the value of *a*, the polar plot will start to rotate in a clockwise direction. Hence, the crossing point on positive real axis will increase but the system is still in stable condition because there is no crossing on negative real axis. This clearly shows that, the effect of sensor dynamics in the frequency response of a single-degree-of-freedom system with acceleration feedback control is unconditionally stable.

### 3.2 Velocity Feedback Control

In the case of velocity feedback control, both of $g_a$ and $g_d$ is set to zero such that (15) can be expressed as

$$G(j\Omega)S(j\Omega)H(j\Omega)=\frac{2\zeta g_v M_s}{CK_s}\left(\frac{j\Omega}{1-\Omega^2+j2\zeta\Omega}\right)\left(\frac{1}{1-(\Omega/\alpha)^2+j2\zeta_s(\Omega/\alpha)}\right) \tag{19}$$

where the real and imaginary part can be separated as

$$\mathrm{Re}\{G(j\Omega)S(j\Omega)H(j\Omega)\}=-\frac{4\zeta g_v M_s}{CK_s}\frac{\left((\Omega\alpha)^2\right)\left(\zeta\left(\Omega^2-\alpha^2\right)+\zeta_s\left(\Omega^2-1\right)\right)}{\left(\left(1-\Omega\right)^2+\left(2\zeta\Omega\right)^2\right)\left(\left(\alpha^2-\Omega^2\right)^2+\left(2\zeta_s\Omega\alpha\right)^2\right)} \tag{20}$$

$$\mathrm{Im}\{G(j\Omega)S(j\Omega)H(j\Omega)\}=\frac{4\zeta g_v M_s}{CK_s}\frac{\left(\Omega\alpha^2\right)\left(\alpha^2-\Omega^2\left(1+\alpha^2-\Omega^2\right)\right)}{\left(\left(1-\Omega\right)^2+\left(2\zeta\Omega\right)^2\right)\left(\left(\alpha^2-\Omega^2\right)^2+\left(2\zeta_s\Omega\alpha\right)^2\right)} \tag{21}$$

Following the same procedure as described earlier in section A, three critical frequencies which are at $\Omega$=0,1 and $\alpha$ are determined. From this result, it can be identified that at $\Omega$=0 the crossing point is at the origin. Meanwhile, at $\Omega$=1 (assume $4\zeta g_v M_s/CK_s=1$) the crossing point is on the positive real axis which is given by

$$\mathrm{Re}^1\{G(j\Omega)S(j\Omega)H(j\Omega)\}=\frac{\alpha^2(\alpha^2-1)}{2\zeta\left(\left(2\zeta_s\alpha\right)^2+\left(\alpha^2-1\right)^2\right)} \tag{22}$$

In contrast, at $\Omega=\alpha$ (assume $4\zeta g_v M_s/CK_s=1$) the crossing point is on the negative real axis, which can be written as

$$\mathrm{Re}^2\{G(j\Omega)S(j\Omega)H(j\Omega)\}=\frac{-\alpha(\alpha^2-1)}{2\zeta_s\left(\left(2\zeta\alpha\right)^2+\left(\alpha^2-1\right)^2\right)} \tag{23}$$

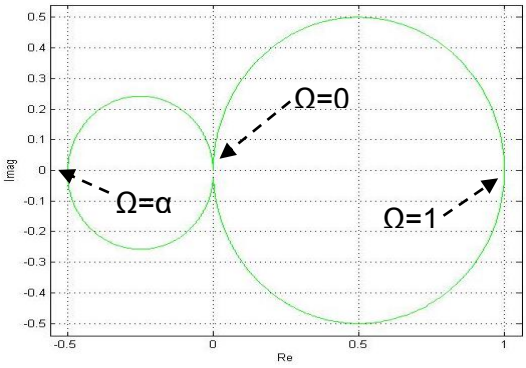


**Figure 6** Polar plot of velocity feedback control with ζ=0.5, $\zeta_s$=0.01 and α=100

For clarity the following parameters are chosen, (ζ=0.5, $\zeta_s$=0.01, $\alpha$=100) in the polar plot of Figure 6. It is clear that the system is conditionally stable, since there is crossing point on the negative real axis, that represents the crossing at the critical frequency, Ω=$\alpha$. In fact, the crossing point is due to the dynamic effect of the sensor.

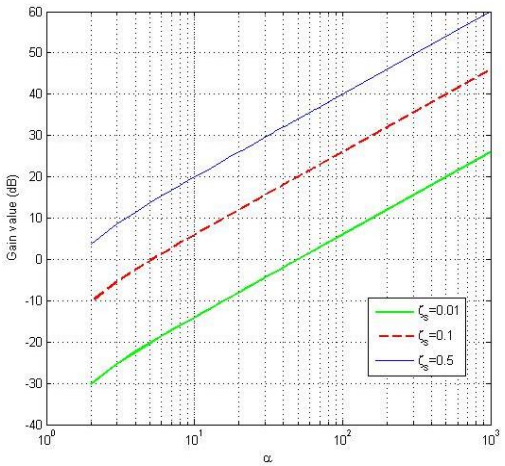


**Figure 7** Graph of maximum gain value (dB) of velocity feedback control (ζ=0.1) with variations of $\zeta_s$ and α

Since the system is conditionally stable, the main concern is to determine its maximum possible gain. The maximum gain $g_{v\_max}$ can be found from the formula

$$g_{v\_\max} = \frac{-1}{\mathrm{Re}^2\{G(j\Omega)S(j\Omega)(H(j\Omega)\}} \tag{24}$$

where $Re^2\{G(j\Omega)S(j\Omega)H(j\Omega)\}$ is the negative real axis crossing point. From this formula, a graph as shown in Figure 7 is plotted to represent the relationship of maximum gain value with $\alpha$. In this graph, the plant damping ratio is set to be constant as $\zeta$=0.1 and with variation of $\zeta_s$. It is observed that the maximum gain value (dB) is linearly dependent on $\alpha$. This relationship can be determined mathematically by simple algebraic manipulation from (24) and (23), to obtain

$$g_{v\_\max} \approx 2\zeta_s\alpha \tag{25}$$

which shows the maximum gain in velocity feedback control is proportional to $\zeta_s$ and $\alpha$.

### 3.3 Displacement Feedback Control

In the case of displacement feedback control, both of $g_a$ and $g_v$ is set to zero such that (15) can be expressed as

$$G(j\Omega)S(j\Omega)H(j\Omega) = \frac{g_d M_s}{KK_s}\left(\frac{1}{1-\Omega^2+j2\zeta\Omega}\right)\left(\frac{1}{1-(\Omega/\alpha)^2+j2\zeta_s(\Omega/\alpha)}\right) \tag{26}$$

where its real and imaginary part may be written as

$$\mathrm{Re}\{G(j\Omega)S(j\Omega)H(j\Omega)\} = \frac{g_d M_s}{KK_s}\frac{\alpha^2\left(\alpha^2-\Omega^2-(\Omega\alpha)^2+\Omega^2\left(\Omega^2-4\zeta\zeta_s\alpha\right)\right)}{\left((1-\Omega)^2+(2\zeta\Omega)^2\right)\left(\left(\alpha^2-\Omega^2\right)^2+(2\zeta_s\Omega\alpha)^2\right)} \tag{27}$$

$$\mathrm{Im}\{G(j\Omega)S(j\Omega)H(j\Omega)\} = \frac{g_d M_s}{KK_s}\frac{2\Omega\alpha^2\left(\zeta\left(\Omega^2-\alpha^2\right)+\zeta_s\alpha\left(\Omega^2-1\right)\right)}{\left((1-\Omega)^2+(2\zeta\Omega)^2\right)\left(\left(\alpha^2-\Omega^2\right)^2+(2\zeta_s\Omega\alpha)^2\right)} \tag{28}$$

By applying the same procedure as described earlier, the system has critical frequency at Ω=0 and $\sqrt{\alpha(\zeta\alpha+\zeta_s)(\zeta+\alpha\zeta_s)}/(\zeta+\alpha\zeta_s)$. By replacing each of these critical frequency into (28), which results crossing point at the origin and negative real axis. In this case, the system is said to be conditionally stable. However, it does not have significant effect on the system stability, because the negative crossing point is occurred at extremely small negative value as shown in Figure 8.

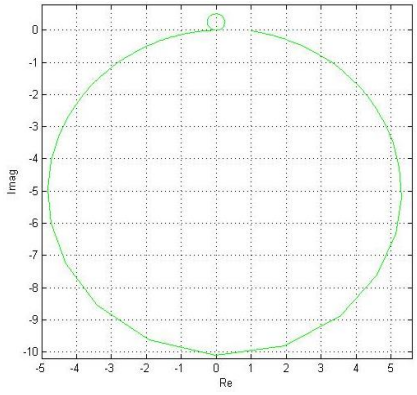


**Figure 8** Polar plot of displacement feedback control with ζ=0.05, ζs=0.01 and α=10

The parameters in Figure 8 are set as the following (ζ=0.05, $\zeta_s$=0.01 and $\alpha$=10) for clarity purpose. The crossing point on the negative real axis can be clearly seen by enlarging the area of the crossing point as shown in Figure 9. It is obvious, the crossing point is occurred at very small negative value.

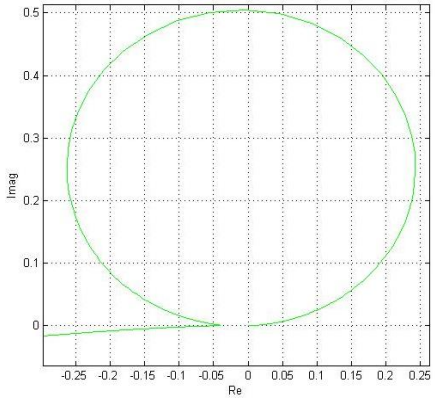


**Figure 9** Zoom of real axis crossing point in Figure 8

By applying the same approach as described in section 3.2, the graph of the maximum gain value for displacement feedback control is plotted in Figure 10. From the graph, it can be seen that the relationship between maximum gain value with at low frequency is nonlinear when $\alpha$<100 for the plotting line of $\zeta_s$=0.01. In this case, at higher frequency where $\alpha$>100, the linear relationship between maximum gain (dB) with $\alpha$ can be determined as

$$g_{d\_\max} \approx \zeta\alpha/\zeta_s \tag{29}$$

In general, based on the derived maximum gain value in (29), the displacement feedback control has its maximum gain value which is proportional to $\zeta$ and $\alpha$, but inversely proportional to $\zeta_s$.

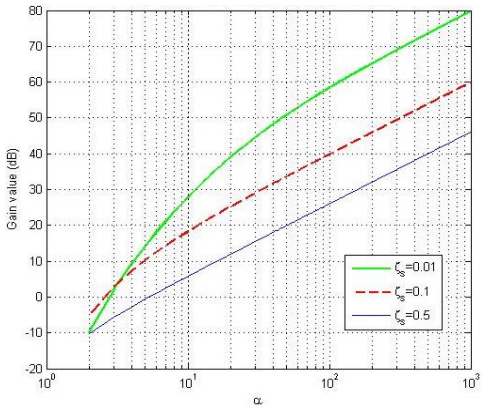


**Figure 10** Graph of maximum gain value (dB) of displacement feedback control ($\zeta$=0.1) with variations of $\zeta_s$ and $\alpha$

## 4.0 DISCUSSIONS

The result from this analysis is presented in the Table 1. For comparison purpose, the Nyquist stability analysis with and without sensor dynamic are presented together. In general, all of the feedback controller types are unconditionally stable without including the sensor dynamics into the system overall transfer function. However, the Nyquist stability results are slightly changed by including the sensor dynamics into the system transfer function. Only acceleration feedback control is maintained with the unconditionally stable result for both cases. However the stability for velocity and displacement feedback control is conditionally stable, by including the sensors dynamic into the overall system transfer function.

The result for velocity feedback control significantly shows that, the crossing point on the negative real axis is mainly caused by the sensor dynamic. The maximum gain for this system is given by $g_{v\_\max} \approx 2\zeta_s\alpha$ .This shows the important role of the sensor damping ratio and the large separation between sensor and plant natural frequency in determining the system stability. The maximum gain is increased when the sensor damping ratio is increased. The same result also true for increasing $\alpha$ that represents the increment of separation between sensor and plant natural frequency.

The result also shown, that the system stability is conditionally stable for displacement feedback control with sensor dynamic. However, it does not have significant effect on the system stability, since the crossing point on the negative real axis is occurred at absolutely very small value.

**Table 1** Results of analysis

| *Control Strategies* | *Nyquist stability analysis without sensor dynamics* | *Nyquist stability analysis with sensor dynamics* |
|---|---|---|
| Acceleration feedback | Unconditionally stable | Unconditionally stable |
| Velocity feedback | Unconditionally stable | Conditionally stable, with $g_{v\_\max} \approx 2\zeta_s\alpha$ |
| Displacement feedback | Unconditionally stable | Conditionally stable, with $g_{d\_\max} \approx \zeta\alpha/\zeta_s$ |

## 5.0 CONCLUSIONS

The stability of a single-degree-of-freedom active vibration isolation system which is based on Nyquist stability criterion has been investigated by including the dynamics of piezoelectric accelerometer into the open-loop transfer function of the system. Three different control strategies which are acceleration, velocity and displacement feedback control has been considered. Simple formulae have been derived which give insight on the frequency at which the system become unstable, and the maximum gain that can be applied to each system. It has shown that the system is only unconditionally stable for acceleration, but is conditionally stable for velocity and displacement feedback control.

## References

[1] A. Preumont. 2002. *Vibration Control of Active Structures*. 2nd edition. Springer.

[2] D. Karnopp, M. J. Crosby, and R. A. Harwood. 1974. Vibration Control Using Semi-active Force Generators. *J. Eng. Ind.* 96: 619-626.
[3] P. G. Nelson. 1991. An Active Vibration Isolation System for Inertial Reference and Precision Measurement. *Rev. Sci. Instrum.* 62: 2069-2075.
[4] S. M. Kim, S. J. Elliott and M. J. Brennan. 2001. Decentralised Control for Multi Channel Active Vibration Isolation. *IEEE Transactions on Control Systems Technology*. 9(1): 93-100.
[5] C. R. Fuller, S. J. Elliott and P. A. Nelson. 1996. *Active Control of Vibration*. Academic Press, New York.
[6] N. S. Nise. 2000. *Control Systems Engineering*. John Willey & Sons.
[7] M.J. Brennan, K. A. Ananthaganeshan, and S. J. Elliott. 2007. Instabilities Due to Instrumentation Phase-Lead and Phase-Lag in the Feedback Control of a Simple Vibrating System. *Journal of Sound and Vibration*. 304(3-5): 466-478.